JASA ARTICLE

On the use of the Lloyd's Mirror effect to infer the depth of vocalizing fin whales

Andreia Pereira,[1,a)] Danielle Harris,[2] Peter Tyack,[3] and Luis Matias[1]
[1]*Instituto Dom Luiz, Faculty of Sciences, University of Lisbon, Lisbon, Lisbon, Portugal*
[2]*Centre for Research into Ecological and Environmental Modelling, University of St. Andrews, St. Andrews, Fife, United Kingdom*
[3]*Sea Mammal Research Unit, University of St Andrews, St. Andrews, Fife, United Kingdom*

ABSTRACT:
The interference between the direct path and the sea surface reflection of a signal as measured by a receiver is called Lloyd's Mirror effect (LME). It results in a frequency-dependent interference pattern that can be observed in a spectrogram. LME depends on the receiver depth, signal source depth, signal frequency, and slant range between source and receiver. Knowing three of these parameters *a priori*, LME can be used to estimate the third parameter, such as source depth. Here, the work in Pereira *et al.* (2016) was expanded to estimate the depth of a vocalizing fin whale recorded by an ocean-bottom seismometer (OBS). In Pereira *et al.* (2016), the depth of a vocalizing fin whale was inferred by manually comparing spectrograms of LME transmission loss models with observed LME. This study developed an automated procedure to perform the same task using the LME interference pattern observed in the spectrograms of the hydrophone and the vertical channel of the OBS. The results show that the joint use of the two channels was the best approach to estimate a source depth using LME. LME provides a non-intrusive approach for estimating the depth at which a fin whale was vocalizing. © *2020 Acoustical Society of America*.
https://doi.org/10.1121/10.0002426
(Received 27 July 2020; revised 6 October 2020; accepted 8 October 2020; published online 25 November 2020)
[Editor: Rebecca A. Dunlop] Pages: 3086–3101

I. INTRODUCTION

Marine mammals rely on sound for different aspects of their life, such as communication, navigation, and foraging (Richardson *et al.*, 1995). Sound has so many functions in the life of marine mammals that researchers can use acoustic data to answer a variety of questions concerning the ecology, physiology, and behavior of these animals. Some marine mammal acoustic signals have characteristics that allow researchers to identify signals at a species level (Watkins, 1981), and sometimes at an individual level (Tyack, 1997). Other signal characteristics can represent information about status and behavior of an animal. For example, geographical differences in sound production and characteristics of signals (obtained from temporal and frequency measurements) among fin whales and blue whales have been suggested as indicators of variation between populations (Hatch and Clark, 2004; McDonald *et al.*, 2006). Further, changes in sound production of several baleen whale species have been associated with a response to changes in the levels of acoustic noise (Parks *et al.*, 2007; Castellote *et al.*, 2012). In this context, an understanding of the acoustic propagation of biological signals in the ocean is crucial for studies of marine mammal sounds that rely on high quality and accurate characterization of the signals. It is crucial to understand whether observed variability in marine mammal signals is biological, i.e., true differences between the signals of conspecifics (or even individual variability), or a result of the effects of acoustic propagation.

On some occasions, acoustic characteristics associated with biological factors might be artefacts of propagation. For example, Premus and Spiesberger (1997) demonstrated that multipath propagation could explain the production of the 20-Hz doublets by fin whales in the Gulf of California. Measurement error might also occur due to acoustic interference caused by sound propagation. For example, inaccurate estimates of sound source levels have been related to the occurrence of acoustic interference (Charif *et al.*, 2002). Although the existence of acoustic interference in recordings of marine mammals' sounds can be detrimental to some analyses, it can also provide opportunities to obtain additional data about the recorded animals, such as range or source depth (Charif *et al.*, 2002).

Fin whales are known to produce a low frequency sound, called the 20-Hz note or regular note, which is a short pulse with an average duration of 1 s or less that sweeps down in frequency from ~30–15 Hz, which means that the instantaneous frequency decreases over time (Watkins, 1981; Hatch and Clark, 2004; Au and Hastings, 2008). This signal is usually repeated with a stereotyped inter-note interval (INI), forming sequences which are grouped in bouts that can last for hours (Watkins *et al.*, 1987; Delarue *et al.*, 2009; Oleson *et al.*, 2014). There are also longer intervals between sequences, defined as rests, which last between 1 and 20 min, and longer gaps, which last between 20 min and 2 h (Watkins *et al.*, 1987;

[a)]Electronic mail: afpereira@fc.ul.pt, ORCID: 0000-0002-5368-5707.

https://doi.org/10.1121/10.0002426

Delarue *et al.*, 2009; Soule and Wilcock, 2012). Fin whales also produce another low frequency sound designated backbeat, which is relatively constant in frequency (between 18 and 20-Hz) and lasts ~0.8 s (Clark *et al.*, 2002). Bouts can be composed exclusively of 20-Hz notes or backbeats, or they can be a mixture of both notes (. Hatch and Clark, 2004; Castellote *et al.*, 2012). The long patterned bouts most likely function as a reproductive acoustic display since, to date, only male fin whales have been observed to produce these sounds, and the production peak of this signal coincides with the breeding season (Croll *et al.*, 2002). It is suggested that male fin whales produce bouts to attract far away females (Watkins 1981; Watkins *et al.*, 1987). Source levels reported for the 20-Hz note range from 159–220 dB *re*:1 μPa at 1 m (Charif *et al.*, 2002; Wang *et al.*, 2016). Propagation models of the 20-Hz note estimate detectable ranges up to hundreds of km in favorable conditions (Payne and Webb, 1971; Hatch and Clark, 2004; Širović *et al.*, 2007). Hydrophones have detected 20-Hz notes up to 185 km away (Northrup *et al.*, 1968; Cummings and Thompson, 1971). The repeated production, low frequency, and high source level of the 20-Hz note show that this signal is adapted for long-distance communication (Tyack, 2000). For animals that can travel over ocean basins, signals that have a long-range propagation can be crucial for their reproduction.

The propagation of the 20-Hz note in the ocean can be modelled by the summation of several rays, the direct path, and multipaths that result from refraction within the water column and reflections off of the boundaries of the sound channel, the sea surface, and the seafloor (Lurton, 2002). For a pressure signal, the reflection coefficient at the sea surface is −1 (i.e., there is 180° phase reversal) for a flat surface. The true value for the surface reflection depends on the frequency of the signal and sea surface roughness. However, attenuation for frequencies lower than 50 Hz is nearly negligible (Hovem, 2013). In contrast, the sea surface acts as a free boundary for particle velocity, and the reflection coefficient will be 1 for a flat surface (perfect reflection) or slightly lower for a rough sea. The seafloor is not a perfect reflector, and its reflection coefficient is more complex than at the sea surface, depending on the signal frequency, incident angle, layering, and elastic properties of the bottom substrate. The reflection coefficient of the seafloor does not involve the phase reversal of the pressure release boundary at the surface. Acoustic interference of a signal occurs when the travel time difference between the direct and one of the multiple paths is less than the signal length. Acoustic interference is stronger when the time difference is on the order of half dominant periods, which correspond to the periods of time with the highest energetic level of a signal (in case of a 20-Hz note these correspond to the middle of the signal). See supplementary material for an example of the results of the interaction between the direct and the multipaths of a synthetic 20-Hz fin whale noted at different slant ranges.[1] In the case of the 20-Hz fin whale notes, when this travel time difference is less than 1 s, it is expected that recorded notes show multipath interference. The resulting interference pattern depends on the geometry of the propagation, water depth, source and receiver depth, slant range, i.e., the horizontal distance between source and receiver, and signal frequency. Given the bandwidth of the 20-Hz note, a full cancellation of the direct path is not expected, but the interference can result in a doubling of the amplitude of the recorded signal (6 dB gain, Charif *et al.*, 2002). The interference from a flat reflector was first presented in the field of optics, and it is known as Lloyd's Mirror effect (LME). The constructive interference that may result from LME, which produces a strengthening of the acoustic signal, has been suggested to be one of the factors that could drive the preferred vocalizing depth for blue whales (Oleson *et al.*, 2007), and the argument may also extend to fin whale vocalizations (Stimpert *et al.*, 2015). In the deep ocean (deeper than 1000 m), LME is observed only when the source (or receiver) is close enough to one of the sound channel boundaries. The depth at which the sound speed is minimum is known as the sound channel axis, and in deep water, it depends mostly on water temperature and pressure (Kerman, 1988). The sound channel axis varies across geographical locations, and can be located at about 1000 m at mid-latitudes to near the surface in polar regions (Etter, 1995). If the receiver is on the seafloor, (as is the case for an ocean bottom seismometer (OBS), LME is due only to the sea surface reflection, and it is an exclusive function of the source depth, water depth, signal frequency, and slant range. Knowing three of these parameters *a priori*, LME can be used to provide an estimate of the fourth parameter, such as signal source depth.

There is a growing concern about the effects of underwater noise on marine life, as levels of background noise as well as peak sound intensity in some areas of the ocean are increasing (Hildebrand, 2009; Kunc *et al.*, 2016). Auditory masking occurs when detection and recognition of one sound are hindered by the presence of another sound (Clark *et al.*, 2009; Erbe *et al.*, 2016). Marine mammals have several strategies to compensate for masking noise, such as an increase in the source level, a change in call frequency or bandwidth, and an increase in call repetition rates (Erbe *et al.*, 2016). If fin whales change the depth at which they vocalize to improve sound propagation properties, then the change of vocalizing depth could represent an anti-masking strategy. Knowledge about depth of vocalizing animals is not only important to understand the effects of anthropogenic pressure on behavior, which potentially affects the fitness and survival of individuals, but can also be important for animal abundance estimation methods (Marques *et al.*, 2013). First, a key parameter of animal abundance methods, the probability of detection may be a function of source depth, e.g., sound propagation models show that the location and width of shadow zones, i.e., zones of low sound intensity, depend on the source depth and the relation with the sound speed depth profile. Second, some animal abundance estimation methods require spatial data, including information about animal depth. For example, distance sampling, one of the most popular abundance estimation methods, estimates detection probability as a function of horizontal range (Marques *et al.*, 2013) and, therefore, requires animal depth

to either be estimated or assumed. Finally, another crucial parameter in some animal abundance estimators is the call production rate, i.e., the average number of calls produced per individual animal over a defined period of time (Marques *et al.*, 2013). Several studies have shown that call production rates vary with depth for several species, such as sperm whales (Thode *et al.*, 2002), right whales (Parks *et al.*, 2011), and fin whales (Stimpert *et al.*, 2015). Therefore, it is important to gather more data about the depths at which animals produce acoustic signals to facilitate animal abundance estimation analyses.

Charif *et al.* (2002) used LME to estimate signal source depth by fitting received sound levels of 20-Hz fin whale notes, and the corresponding source-to-receiver horizontal distances to a LME transmission loss (TL) model. However, the estimated depths of the 20-Hz notes were not consistent, and the authors attributed the poor performance to the small number of hydrophones used (Charif *et al.*, 2002). Pereira *et al.* (2016) developed an exploratory analysis to estimate the depth of a vocalizing fin whale by manually comparing spectrograms of LME TL models with spectrograms of the LME recorded in a fin whale bout. The dataset comprised one bout recorded in the Gulf of Cadiz by a 4 channel OBS that contained a hydrophone and a vertical geophone (in addition to two horizontal geophones whose data were not used). In this study, the work presented in Pereira *et al.* (2016) was expanded by automating the procedure to compare synthetic and recorded spectrograms showing LME interference. In addition, this study shows an alternative approach to Charif *et al.* (2002) by demonstrating the use of LME in a single receiver to infer the depth of a vocalizing fin whale.

II. METHODS

A. Recording instruments and dataset

The Gulf of Cadiz, Southwest of Iberia (Fig. 1), is recognized as a source area of potentially destructive earthquakes and tsunamis, such as the 1 November 1755 Lisbon earthquake (Silva, 2017). To investigate the current seismic activity in the area, the NEAREST project (integrated observation from NEAR shore sourcES of Tsunamis (T): towards an early warning system) deployed a temporary network of 24 OBSs that recorded continuously for nearly one year, between August 2007 and July 2008 (Geissler *et al.*, 2010; Silva, 2017). The OBSs were equipped with Güralp CMG-40T broadband seismometers (Güralp Systems Ltd., Aldermaston, England), and High-tech HTI-04-OBS PCA/ULF hydrophones (High Tech, Inc., Long Beach, MS, USA), allowing for the recording of the 3-component ground motion (two channels for the horizontal components, X and Y, and one channel for the vertical component, Z), and the sound pressure in the water (H-channel), all with a sampling rate of 100 Hz. In addition to the earthquakes, these instruments also recorded fin whale vocalizations including the 20-Hz classic and backbeat notes described in Sec. I. These recorded vocalizations have been used to detect and track fin whales (Matias and Harris, 2015), for density estimation (Harris *et al.*, 2013), and to characterize fin whale 20-Hz notes (Pereira *et al.*, 2020).

The 20-Hz fin whale notes were identified using a modified normalized cross-correlation equation with a matched filter of the signal waveform (Harris *et al.*, 2013; Matias and Harris, 2015). More details about the automatic detection process are given in Harris *et al.* (2013), Matias and Harris (2015), and Pereira *et al.* (2020). Although backbeat notes were observed in the recorded fin whale bouts, they were not considered for the analysis. The resulting detections were confirmed using spectrograms calculated with TRITON (Wiggins *et al.*, 2010), a software package written in MATLAB (MathWorks, 2010). Spectrograms were calculated using the Z-channel data because the vertical seismometer channel showed higher signal–to–noise ratio when compared to the H-channel recordings, a feature that is also observed in other published studies (McDonald *et al.*, 1995). Spectrograms were computed using a discrete Fourier transform with a Hanning window. Equalization, brightness, and

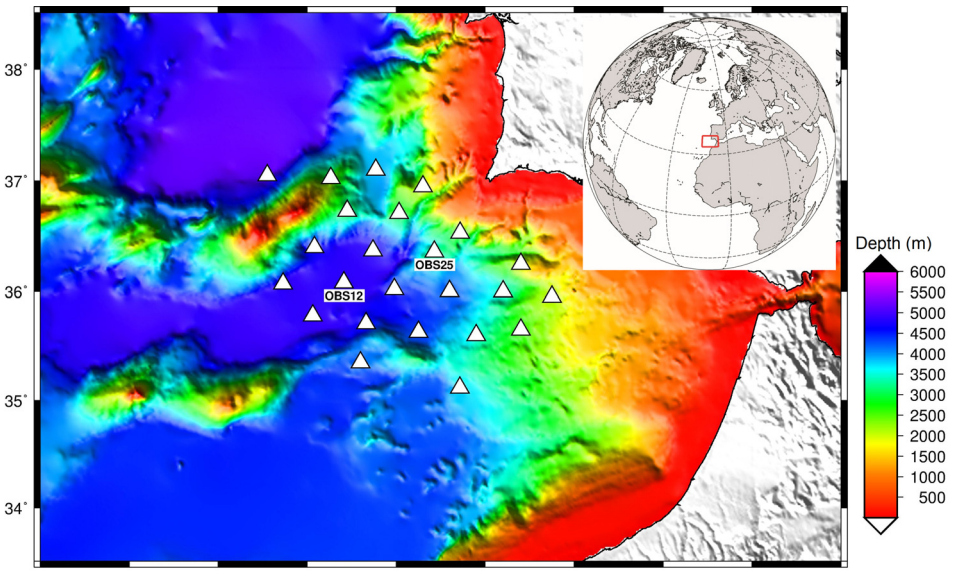

FIG. 1. (Color online) Location of the NEAREST OBS network. The color bar indicates depth of the seafloor. The station whose data was used in this work is OBS12. The sound speed profile used in this work was obtained from a CTD cast located close to OBS25.

https://doi.org/10.1121/10.0002426

contrast settings were adjusted to produce the best visual spectrographic image. During visual data analysis of spectrograms, several fin whale bouts showed clear interference patterns that were indicative of LME (Pereira *et al.*, 2016). One of the strongest bouts recorded by OBS12, which was deployed at 4860 m (Fig. 1) on 9 November 2007 from 01:00–03:00 (Pereira *et al.*, 2016), was chosen to exemplify the use of LME to infer the depth of the vocalizing whale. Twenty-Hz notes only last ∼1 s, so they occupy only a small portion of the total bout duration; the remainder of the bout duration is comprised of varying levels of background noise (Fig. 2).

The visualization of the interference patterns and the modelling of the LME were facilitated by the development of a compressed time series containing only 20-Hz notes from the sampled bout. All the 20-Hz notes of the bout were extracted using a time window of 1.1 s around each note, starting 0.05 s before the matched filter trigger time. The spectrograms of the H- and Z-channels of this new time series, also known as composite spectrograms, were constructed in TRITON with a window length of 256 samples (2.56 s at a sampling of 100 Hz), a Hanning window taper, and 95% overlap (implying a 0.128 s shift between each spectrum calculated for the spectrogram). Contrary to the detection process, in this step the Z- and the H-channels were both used because the LME pattern was expected to differ across the two channels (the reflection coefficient on the sea surface has opposite signs). Since the resolution of the spectrum of the composite spectrograms of the two channels was low (the frequency spacing was 0.391 Hz), both spectrograms showed small horizontal bands that were not related with the interference pattern (Fig. 3). When 20-Hz notes are produced in sequences, the composite spectrogram is expected to show a frequency band with the same frequency limits of 20-Hz notes, and similar levels of intensity throughout the band. However, the time and frequency characteristics of notes are changed when the surface-reflected path superimposes with the direct path of the note. This results in visible curved interference patterns in the composite spectrograms of the recordings, which create a symmetrical "U" shape characteristic of the LME pattern (Hudson, 1983). Both H- and Z-composite spectrograms showed clear interference patterns (Fig. 3) but, as expected, these did not coincide, because of the opposite sign of the surface-reflection coefficient.

In the investigated bout there was a dominant INI from the automatic detection process of 13.5 s (SD = 0.2 s) (Fig. 3), but there was also an INI of 27.0 s (SD = 0.8 s) that was visually confirmed afterwards as notes missed by the automatic detector. The INI plot showed a regular pattern of longer more variable intervals, identified in Sec. I as gaps, which lasted between 186 and 246 s. The occurrence of these gaps was interrupted by a longer interval, a rest, with a duration of ∼30 min. After the rest, it was possible that a new whale started the bout. However, the estimates of the slant ranges of the notes (presented below in Sect. II B) showed that they were produced at similar slant ranges, strongly suggesting they were produced by the same whale. Therefore, notes after the rest were also used in the following analysis. If the gaps are interpreted as surface breathing periods between dives (Payne and Webb, 1971), then the INI sequence showed at least six very stereotyped dives with a minimum duration (computed from the initial and final call times) of 12.1–14.5 min. The analyzed bout also included two incomplete dives at the start and end of the sequence, and two additional presumed incomplete dives interrupted by the 30 min rest that may mark, or not, the end and start of one dive.

B. Estimating the slant range to the sound source

To apply LME modelling to infer the source depth (Z_S), all other parameters described in Sec. I must be known or estimated. The receiver depth was measured at 4860 m but the slant range, i.e., direct distance between the sound source and the receiver, needs to be estimated. In this case, the fin whale bout investigated was recorded by a single instrument and, as such, two ranging methods could be applied: the multipath based technique (Wilcock, 2012; Weirathmueller *et al.*, 2017) or the single station method (SSM) proposed by Matias and Harris (2015). The SSM is limited to short slant ranges because the method can only be applied when the incidence angle at the sea bottom is smaller than a critical incidence angle, which is a function of the sound speed in the water and the P-wave seismic velocity at the seafloor. This appropriate incidence angle only occurs for slant ranges typically on the order of the

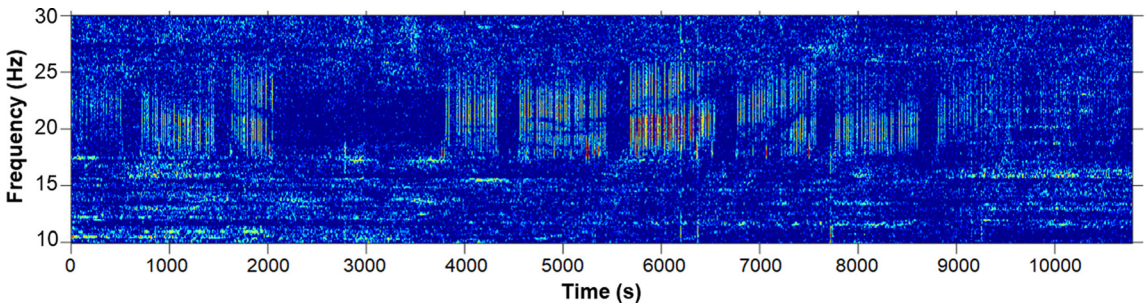

FIG. 2. (Color online) Spectrogram showing 3 h of the fin whale bout recorded by OBS12, on 9 November 2007 and starting at 01:00. The frequency dependent interference pattern is evident in some notes. Backbeats (signals around 18 Hz) were also observed but were not considered for the analysis. Spectrogram parameters: frame size – 1024 samples, 95% overlap, Hanning window, equalized. Sampling rate was 100 Hz.

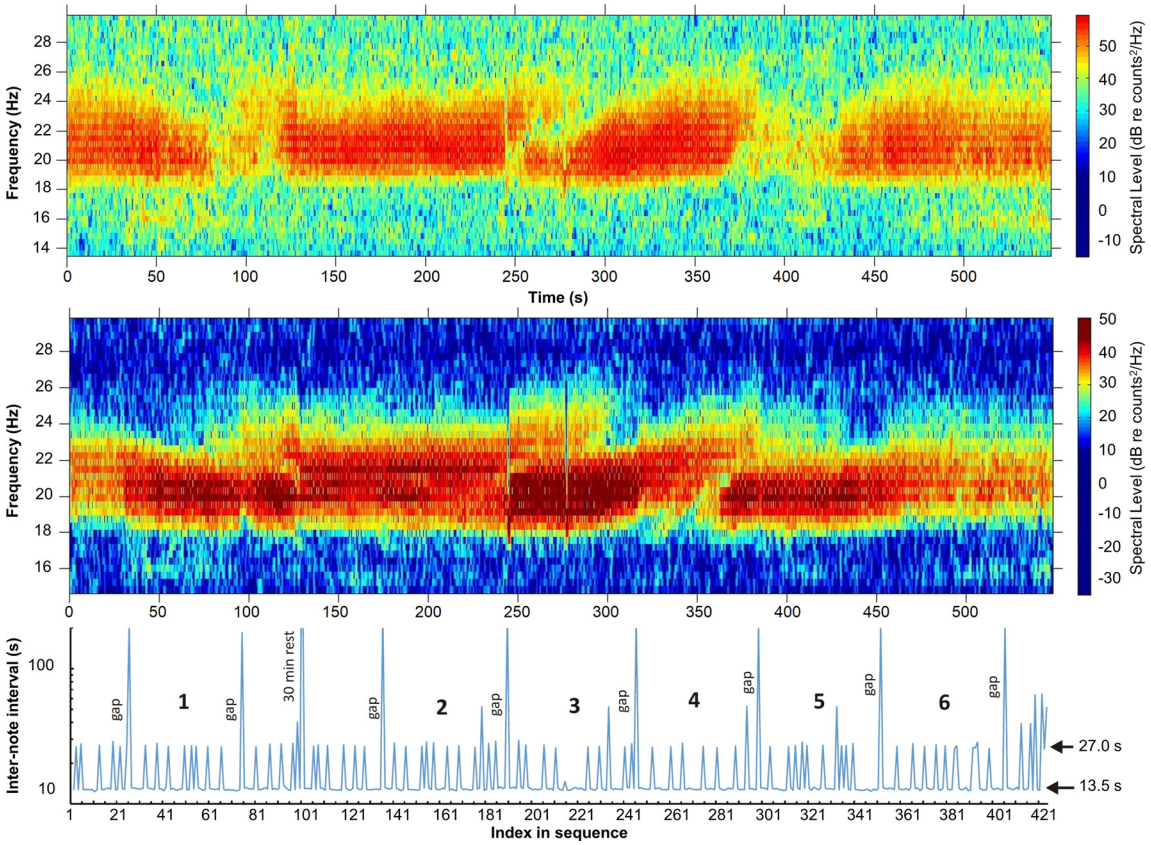

FIG. 3. (Color online) Composite spectrogram of the fin whale bout without periods of silence computed from 100 Hz sampled data. (a) for the hydrophone channel and (b) for the vertical component of ground velocity. Spectrogram parameters: Frame size – 256 samples, 95% overlap, Hanning window, not equalized. (c) Inter-note interval on a logarithmic scale to show the regular sequences interrupted by gaps and one longer rest. The numbers mark the inter-gap intervals, which represent our assumption of six stereotyped dives.

ocean depth (Matias and Harris, 2015). Preliminary evaluation of the estimated slant ranges of the fin whale notes in the selected bout in this study showed that presumed slant ranges were close to and likely exceeded the maximum estimable range of 7300 m, defined by the critical angle of 56.44°, so the multipath method was used for slant range estimation. However, multipath amplitudes of the investigated bout were very weak, and their relative timing to the direct path could not be measured with confidence using the raw data. For this reason, a new methodology was developed to enhance the multipath detection which is described below.

The data recorded by the Z-channel (which was the channel used for the detection and ranging process) were processed in a standard seismic processing software (Parallel Geoscience, 1999) in the following sequence. i) Reformatting data to SEG-Y in which each note is an individual waveform with traces aligned according to its trigger time. ii) Realignment in time of the direct path notes with residual statics, which is a seismic processing tool that uses cross-correlation between each waveform, and a "pilot" trace to correct for small time differences between traces, since the direct path of the several notes of the bout were not perfectly aligned in time. With all notes perfectly aligned, the multipaths were expected to be more coherent in their arrival time, facilitating their identification. iii) Computation of instantaneous amplitude (signal envelope) by Hilbert transform, which transformed the 20-Hz notes into smooth half-sine curves, improving the identification of the multipath arrival times. iv) Bandpass filter between 0.4 and 2.0 Hz to enhance the signal envelope with ∼0.8 s duration, and transform each note into one sinusoidal cycle, with one large positive and one smaller negative oscillation. v) Amplitude equalization using automatic gain control with 1000 ms window to facilitate the picking of the low amplitude multipaths of the 20-Hz notes. Figure 4 shows the result of this processing, and the smooth continuous lines picked for the direct and multipath arrivals. Not all multipath arrival times could be identified in the investigated bout, even after the signal processing treatment. Therefore, further analysis of LME was restricted to 424 fin whale notes for which slant range could be estimated.

The time difference between the direct and multipath of the signal was used to estimate the slant range of the 20-Hz notes. For this purpose, the ray paths and travel times of both signals were considered: the direct one generated at some assumed source depth; and the multipath, including two additional paths, one reflecting at the sea surface and the other at the sea bottom. The sound propagation modelling was conducted assuming a vertically stratified ocean

https://doi.org/10.1121/10.0002426

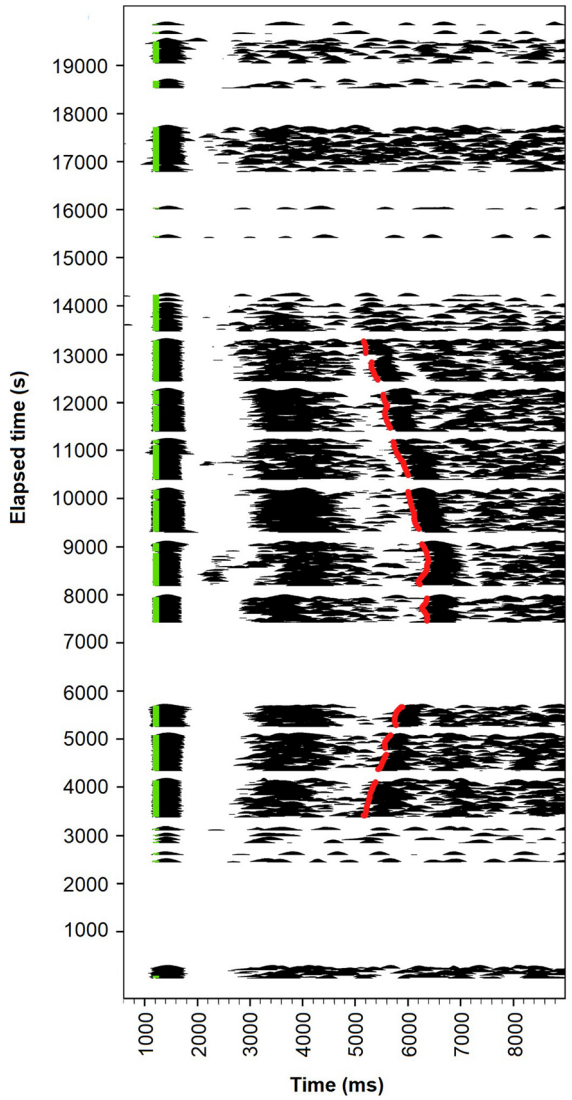

FIG. 4. (Color online) Display of the 20-Hz fin whale notes side-by-side after applying the processing sequence with SPW (Z-channel). The vertical axis represents elapsed time. The colored lines show the arrival times picked for the direct (green) and multipath (red) notes.

that is isotropic in the horizontal plane with sound speed properties computed from conductivity, temperature, and depth (CTD) data recorded on 24 August 2007 as part of the EC-NEAREST project (Lobue, 2012, see supplementary Fig. 3[1]) at a location close to OBS25 (Fig. 1). The estimated slant ranges of each note of the investigated bout transited between 6.2 and 11.6 km away from the receiver during the duration of the bout.

Several assumptions were required to estimate the slant range between the fin whale notes and the OBS. First, the sound speed profile of the area was assumed to be the same as the CTD data obtained at a different location (OBS25) and at a different day than the recorded fin whale bout. The uncertainty related to this is difficult to evaluate. However, a comparison between heterogeneous (using the sound speed profile obtained with the CTD data) and homogeneous (considering an average sound speed) propagation models suggests that this uncertainty would be unlikely to alter slant range estimates by >100 m. Second, the sea bottom was assumed to be flat around the OBS location. For deep ocean conditions and a shallow sound source, the first multipath is reflected at the flat sea bottom at a distance ~2/3 of the slant range. The flatness assumption was confirmed by the inspection of the detailed multibeam bathymetric data (Zitellini *et al.*, 2009) around the OBS12 location. The bathymetry was flat, and the relief did not exceed 20 m inside the radius of the maximum estimated range. For the sound propagation modelling, a fixed depth of 50 m for the sound source was also assumed, a parameter that was unknown. Comparing the estimated slant ranges, assuming source depths of 0 and 200 m, the differences in estimated values for a 6 km range (considering the same travel time difference) are 60 and 250 m, respectively. These differences increase to 400 and 700 m, respectively, for an estimated slant range of 12 km. These values should be considered as maximum estimates of the uncertainty that result from the unknown value of the vocalization depth.

There were difficulties in detecting and timing the multipath arrivals, even after enhancing the multipath signals with SPW (Parallel Geoscience, 1999). The measurement error in picking the multipath arrival times was estimated to be random and less than ±0.1 s. The consequences of this error were evaluated by computing the variation in slant range due to such errors. At close slant ranges (<3 km), the uncertainty resulting from a timing error of 0.1 s was high, greater than 500 m. Between 3 and 12 km the error was typically 400–500 m. For larger slant ranges, the estimated error also increased steadily to 1 km for a 20 km range. To reduce this uncertainty, we took advantage of the fact that notes are produced in sequences, and during each sequence, the whale is not expected to change the speed suddenly or have very high speeds. The random error that resulted from estimating the times of multipath arrivals is reduced by smoothing the initial estimates of slant ranges using the following procedure. The input data were a series of N slant ranges and origin times, X_i (origin time) and T_i (detection time). With these we computed the slant speed, V_i, as

$$V_i = \frac{X_i - X_{i-1}}{\Delta T_i} \quad for\ i = 2, \ldots, N \quad \Delta T_i = T_i - T_{i-1}. \tag{1}$$

Next, we sought the corrections for the slant ranges as

$$X'_i = X_i + \Delta X_i \quad so\ that \quad V'_i = \frac{V_i - V_{i-1}}{2} \quad and \quad \sum_{2}^{N} \Delta X_i = 0. \tag{2}$$

Initializing the first correction to 0, the other corrections were obtained by the recursive expression

$$\Delta X_i = \Delta X_{i-1} - \frac{X_i}{2} + \frac{X_{i-1}}{2}\left(1 + \frac{\Delta T_i}{\Delta T_{i-1}}\right) - \frac{X_{i-2}}{2}\frac{\Delta T_i}{\Delta T_{i-1}} \quad for\ i = 2, \ldots, N. \tag{3}$$

The condition that the sum of all corrections is zero was adjusted as the final step.

C. LME modelling

The methodology described below is general, and can be applied to any dataset of 20-Hz notes when a slant range is known. Since the recording instrument is at the seafloor (at depth Z_R), only the interference that occurs between the direct and surface reflected sound when the sound source is at a depth Z_S was considered (Urick, 1967). As mentioned in Sec. I, when the receiver is at the seafloor, LME is only a result of the sea surface reflection. Attenuation due to geometrical spreading of the sound was considered to be proportional to $1/R^2$ (R is the distance between source and receiver), without considering the frequency dependent attenuation effects (Brekhovskikh and Lysanov, 1982), which are negligible for the low frequencies investigated. For an emitted monochromatic pressure wave p (frequency f) propagating in a medium with constant sound speed (c_w), the following expression is derived for the recorded signal

$$P(r,Z_R,Z_S,f) = \frac{e^{ikR_1}}{R_1} + \mu\frac{e^{ikR_2}}{R_2} \quad k = \frac{2\pi f}{c_w}. \tag{4}$$

In this expression, r represents the slant range, R_1 and R_2 are the distances travelled by the direct and reflected sounds, respectively (that depends on r, Z_R, Z_S), and μ is the surface reflection coefficient. For a pressure wave and ideally flat sea surface, the surface reflection coefficient should be $\mu = -1$, and for the vertical particle motion (as recorded by a seismometer) on the same conditions it should be $\mu = 1$. The roughness of the sea causes the surface to both reflect and scatter sound, with the consequence that less energy will be reflected. If θ is the grazing angle of the incident ray on the surface, λ is the acoustic wavelength, and σ_h is the root-mean-square (RMS) surface wave height, then the surface reflection coefficient can be approximated by (Hovem, 2013)

$$|\mu| = \exp\left[-2\left(\frac{2\pi}{\lambda}\sigma_h \sin\theta\right)^2\right]. \tag{5}$$

The investigated bout was recorded in November, a period when storms can affect the Gulf of Cadiz significantly, thus increasing the sea roughness and decreasing the sea surface reflection coefficient. In the absence of buoy measurements of wave height close to the recording OBS, the model predictions by *Instituto Hidrográfico* that runs the SWAN model (Simulating WAves Nearshore wave model) as described by Booij *et al.* (1999) were used. The model provides estimates for significant wave height (SWH), and the mean wave period for any location inside a defined prediction area. On the day of the investigated bout, 9 November 2007, the SWH predicted did not exceed 1.4 m. The RMS wave height was estimated from SWH by $\sigma_h = SWH/\sqrt{2}$ (Holthuijsen, 2010), which resulted in 1 m for the period of observations. Under this sea condition, the surface reflection coefficient for the following modeling processes was assumed to be $|\mu| = 1$.

To model LME on spectrograms, Eq. (4) was used, and the interference results in terms of TL expressed in dB by

$$TL(r,Z_R,Z_S,f) = -20\log_{10}\left(\frac{P}{P_{ref}}\right), \tag{6}$$

where P_{ref} is the reference sound pressure taken to be 1 μPa.

TL models and figures were developed using a modified version of the MATLAB code presented in Thompson (2009). Taking into consideration the bandwidth limits of the 20-Hz fin whale note, a cosine taper between 16 and 18.5 Hz at the low end, and between 25 and 28 Hz at the high end was applied to the spectrograms to improve the resolution. Figure 5 shows spectrograms for the Z- and H- channels obtained from the outlined model for slant ranges up to 12 km, with the fixed receiver depth for OBS12 (4860 m), and for 3 representative source depths, 20, 50, and 100 m. LME was clearly identified by the negative interference bands, visible as blue on the color scale, which represented high TL levels (Fig. 5). These bands only appeared at small intervals of slant ranges with large range intervals in between where LME was absent. Non-LME ranges dominated for shallow source depths, and there were no slant ranges with LME visible in the H-channel spectrograms for 20 m source depth. The source depth dependence of LME was better appreciated when the TL was plotted for a fixed reference frequency (20 Hz) and changing source depths, between 0 and 300 m, as shown in Fig. 6. No LME was visible for hydrophone recordings at slant ranges larger than 5000 m and source depths shallower than 50 m (Fig. 6). At short slant ranges, LME was only seen for source depths deeper than 30 m for both channels. The vertical seismometer signal was affected by LME at short slant ranges for source depths as shallow as 10 m. Both figures show that LME was more useful for inferring sound source depth when both H– and Z–channels were available, and that a large interval of slant ranges is available (e.g., 5000 m or larger). The synthetic spectrograms were computed for source depths from 10–300 m every 2 meters. This short interval was required to capture the variability of LME on the spectrograms, particularly below 40 m source depths.

F. Estimating the source depth from spectrogram-correlation

The depth of the vocalizing fin whale was estimated by comparing the power spectrogram (in arbitrary dB units) of the investigated bout, $S(t_j,f_i)$, with a series of synthetic spectrograms, $M_n(t_j,f_i)$, representing the TL computed from Eq. (6) for a fixed receiver depth, and a series of source depths identified by the index n, using the same slant ranges that were computed for the investigated bout. The signal time and frequency intervals were the same between observed and synthetic spectrograms. The most straightforward measure of

https://doi.org/10.1121/10.0002426

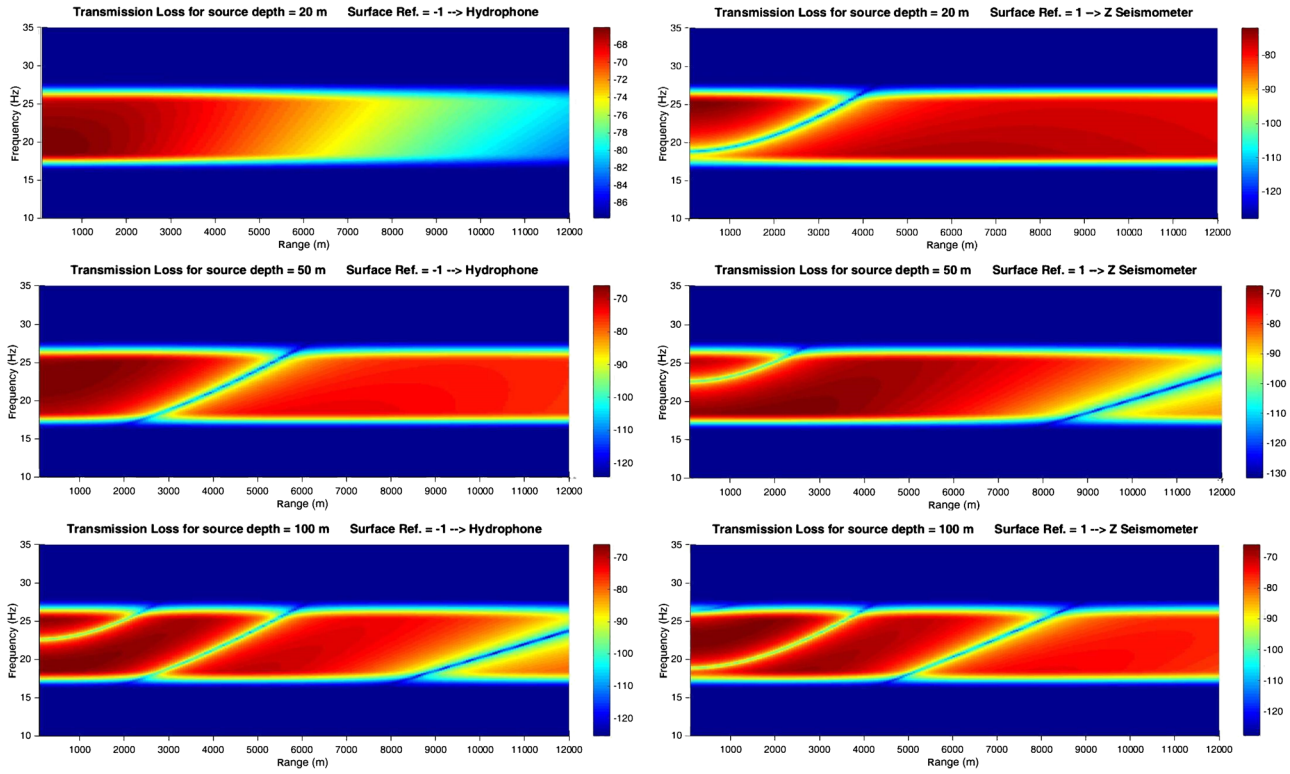

FIG. 5. (Color online) Synthetic spectrograms for TL (dB) computed from Eq. (6). Receiver depth is 4860 m. Three representative source depths are presented, 20, 50, and 100 m, H-channel on the left and Z-channel on the right.

similarity between the recorded spectrogram and one model n is the spectrogram correlation, C1:

$$C1_n = \frac{\sum_{i,j} S(t_j,f_i)\, M_n(t_j,f_i)}{\sqrt{\sum_{i,j} S(t_j,f_i)^2 \sum_{i,j} M_n(t_j,f_i)^2}}. \tag{7}$$

The spectrogram correlation varies between -1 and $+1$, and the model with the highest correlation value is assumed to be the most similar to the observations. Since the 20-Hz fin whale notes are band-limited signals, we limited the computation of the spectrogram correlation between 18 and 25 Hz. Matias and Harris (2015) showed that the 20-Hz note amplitude did not precisely follow the 1/R attenuation law as modelled in Eq. (4). To mitigate this issue, a second spectrogram correlation, C2, was computed in order to avoid the bias in correlation from large differences in absolute amplitudes due to geometrical spreading:

$$C2_n = \overline{C2_{n,j}} \quad with \quad C2_{n,j=} \frac{\sum_{i} S(t_j,f_i)\, M_n(t_j,f_i)}{\sqrt{\sum_{i} S(t_j,f_i)^2 \sum_{i} M_n(t_j,f_i)^2}}, \tag{8}$$

where $C2_n$ is the average spectrogram correlation of all 1-D correlations computed at each time frame. The use of Eqs. (7) and (8) resulted in high values of spectrogram correlation for all models tested ($>$0.976), and the best model was the one built from with a sound source depth of 10 m without any visible LME interference pattern in the spectrogram. Several additional signal processing steps were required to interpret these results for estimating source depth.

First, the model spectrograms were smooth (Fig. 5), while the observed ones (Fig. 2) showed a banded pattern that resulted from the frequency sampling of the discrete Fourier transform applied to 256 samples of data. Furthermore, the Thomson (2009) model applied in Eq. (6) does not consider that the 20-Hz fin whale note is a short pulse with a frequency down sweep. To generate more realistic model spectrograms, the interference pattern in the time domain was computed using a synthetic waveform for the 20-Hz note provided by Mellinger (2015) (see supplementary Fig. 11). The reflected signal was generated by shifting the master waveform in time according to the time shift computed from the sound propagation model. The amplitude of the reflected signal was multiplied by the surface reflection coefficient, and both primary and reflected signals were attenuated assuming $1/R^2$ geometrical spreading. To avoid any problems due to sampling at 100 Hz and to the short duration of the pulse, the initial time series was expanded on both sides, adding 150 samples, and then the signal was interpolated to 1000 Hz. The sum was made at 1000 Hz, and the composite signal was finally decimated to 100 Hz.

Second, both spectrograms, observed and modelled, were strictly positive functions. Thus, it is natural that, without negative values, the spectrogram correlation would

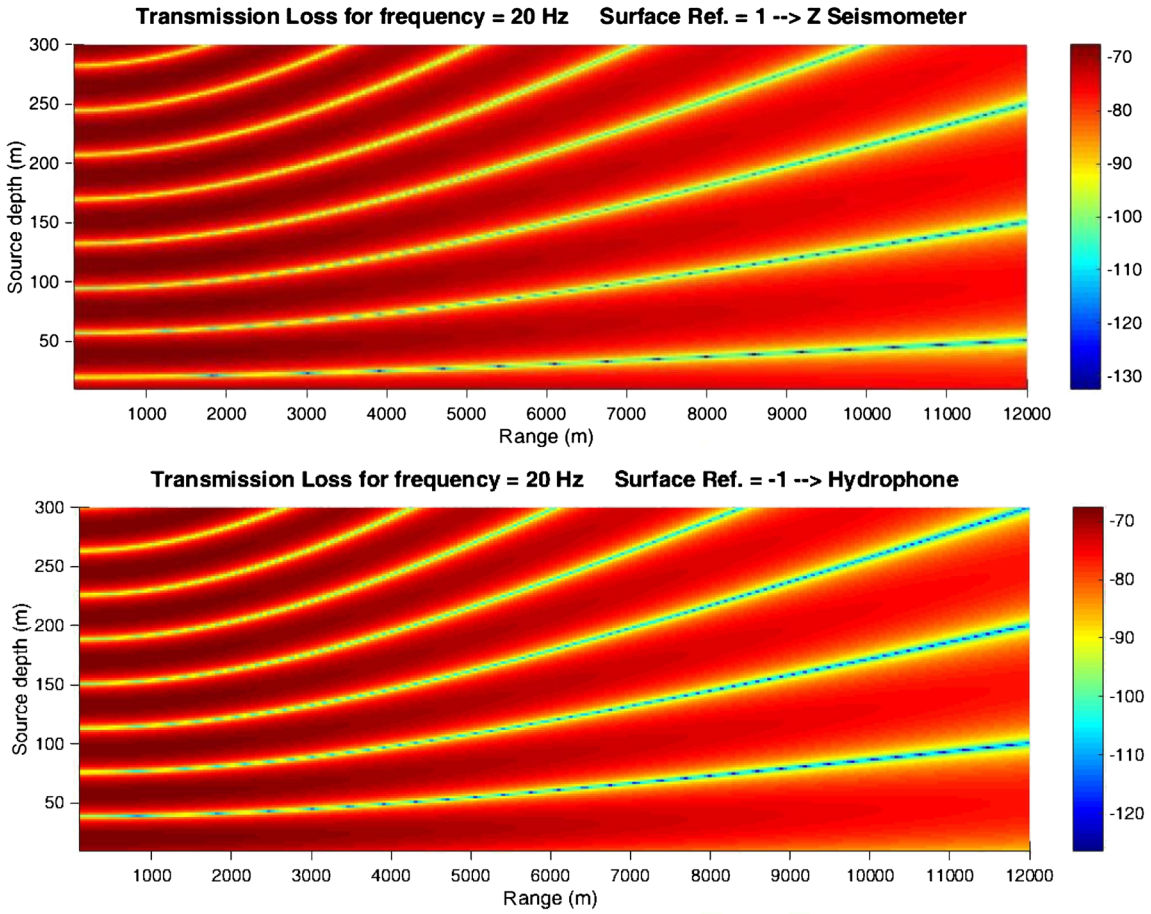

FIG. 6. (Color online) Transmission loss in dB, resulting from LME computed for a frequency of 20 Hz and variable source depths. Top H-channel, bottom Z-channel.

always result in high values. Spectrogram correlation results may not match the spectral features detected on a visual inspection of the spectrograms. To improve on this, the spectrogram correlation computation was modified to use a scaled version of the spectrograms. The observed spectrogram values $S(t_j,f_i)$ were displaced by the median inside the frequency window of interest (18–25 Hz):

$$\hat{S}(t_j,f_i) = S(t_j,f_i) - median[S(t_j,f_i)]. \quad (9)$$

The same procedure was applied to the model spectrograms, this time with a constant value α so that all models were scaled equally, disregarding the effects on total power that the interference patterns may cause.

$$\hat{M}_n(t_j,f_i) = M_n(t_j,f_i) - \alpha. \quad (10)$$

The constant α of 50 dB was chosen because it resulted in more estimated depths.

Finally, the negative influence that the horizontally banded structure of the observed spectrograms might have upon the spectral correlation parameters was addressed. For this purpose, smoothed versions of the observed and synthetic spectrograms resampled on a regular grid with cells 1 s $\times$ 0.2 Hz in size were generated, performing a total of 443 $\times$ 246 cells. The effectiveness of this procedure can be seen by comparing the spectrograms for the H-channel shown in Figs. 3 and 8.

III. RESULTS

A. Estimating the depth of the vocalizing whale

The methodology described in Sec. II was applied to one fin whale bout, and the spectral correlation functions C1 and C2 were computed for models with variable source depth, using the smoothed and scaled version of the spectrograms for the H-channel (Fig. 7). Both C1 and C2 showed high correlation values for very shallow source depths where no LME interference was observed. Because of the lack of LME patterns in the spectrograms, the models computed with shallow source depths were discarded. For source depths larger than 10 m, the maximum of C1 and C2 was attained for a source depth of 72 m.

The spectrograms of observed data and the best model are shown in Fig. 8. The similarity between both spectrograms is clear. Both the observed and the best model spectrograms showed the same energy band between 18 and 25 Hz. The negative interference features caused by LME in the observed spectrogram at ~60–100 and ~300–350 s,

https://doi.org/10.1121/10.0002426

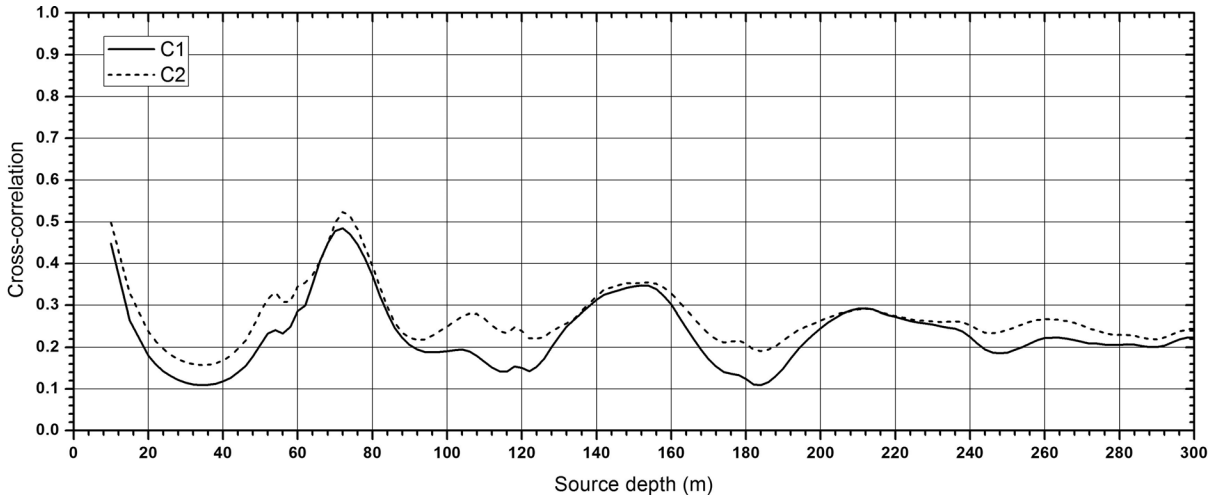

FIG. 7. Spectrogram correlation between the spectrogram of the H-channel and the model spectrograms. C1 values are represented with the solid curve, and C2 values are represented with the dashed curve. The best model was calculated with a source depth at 72 m.

which are represented by the cooler colors, were also observed in the model spectrogram. However, the observed spectrogram showed an interference feature between times 210 and 220 s that was not explained by the model.

The same procedure was applied to the Z-channel spectrograms. The corresponding C1 and C2 correlation functions are shown in Fig. 9. As before, C1 and C2 were very large at shallow source depths where no LME interference was observed. Two maxima could be identified for deeper sound sources, one at 72 m for C1 and another at 76 m for C2. Comparing the spectrograms of the observations with the best model (72 m, Fig. 10), the overall amplitude variation on the observed spectrogram was captured by the model but there was no clear LME interference pattern for this source depth in the model.

Given that the Z- and H-channels provide LME interference patterns that are different, the previous results were combined to provide a joint evaluation of the best source model. The geometrical and arithmetic averages of the two spectrogram correlation functions are shown in Fig. 11. This

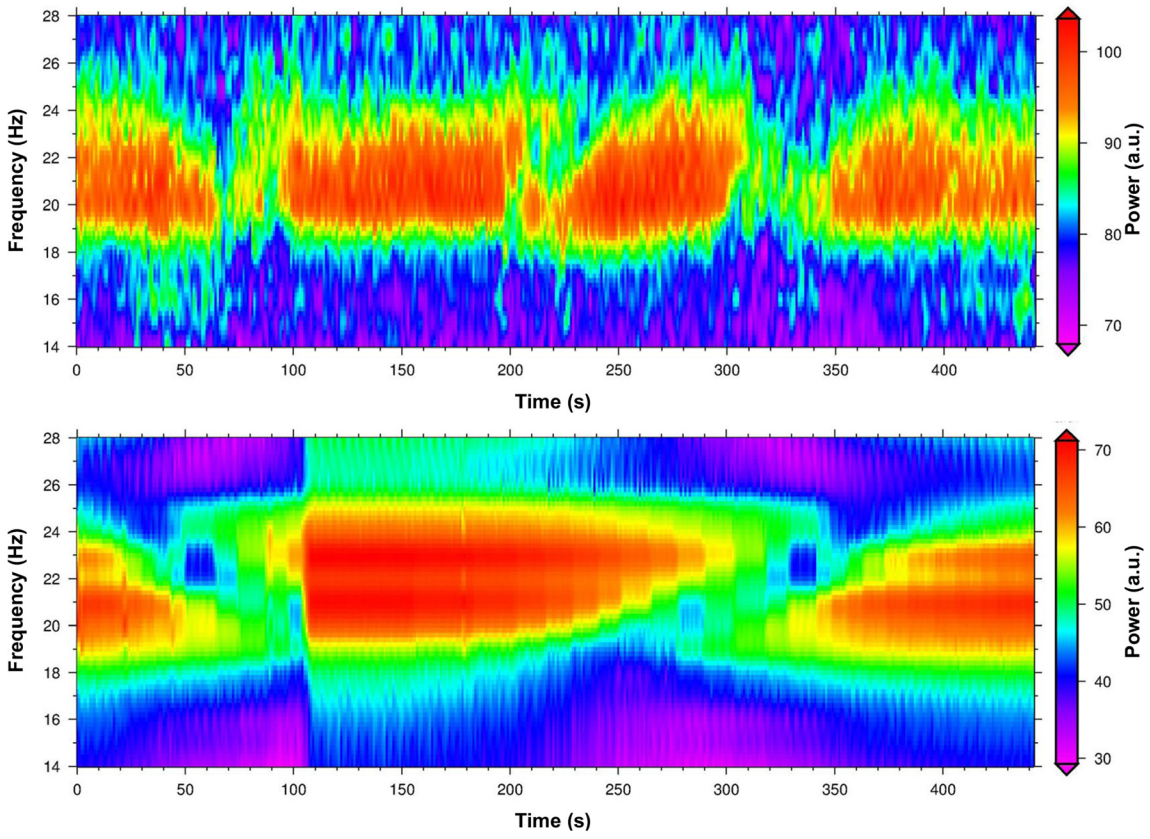

FIG. 8. (Color online) Smoothed spectrograms of the observed fin whale bout in the H-channel (top) and the model for a source depth at 72 m (bottom).

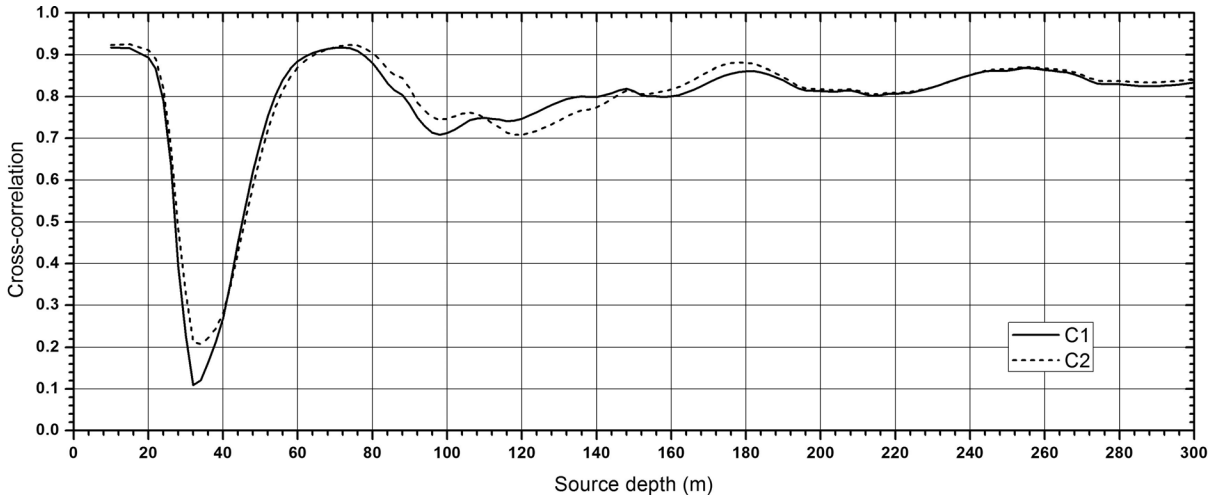

FIG. 9. Correlation between the spectrogram of the Z-channel and the model spectrograms. C1 values are represented with the solid curve, and C2 values are represented with the dashed curve. The best model for C1 was calculated with a source depth at 72 m, while the best model for C2 was calculated with a source depth at 76 m.

combination showed a clear preference for a source depth at 72 m. Other relative maxima that appeared on the Z- or H-channel spectrogram correlations were now subdued due to the opposite effect of the correlations of the two channels.

B. Effect of slant range bias in the inference of depth

To estimate the source depth using the LME approach, the slant range to each fin whale note must be known. As discussed in Sec. II B, the multipath technique used for this computation may introduce up to 400–500 m measurement error for slant ranges between 3 and 12 km, which include the estimated slant ranges of the 20-Hz notes (6.2–11.6 km). However, since a smoothing procedure was applied to the estimated slant ranges to avoid unrealistic whale displacement speeds, this error was not expected to be random but, instead, a systematic behavior, and it may be nearly constant for all the slant ranges investigated. To evaluate the effect of

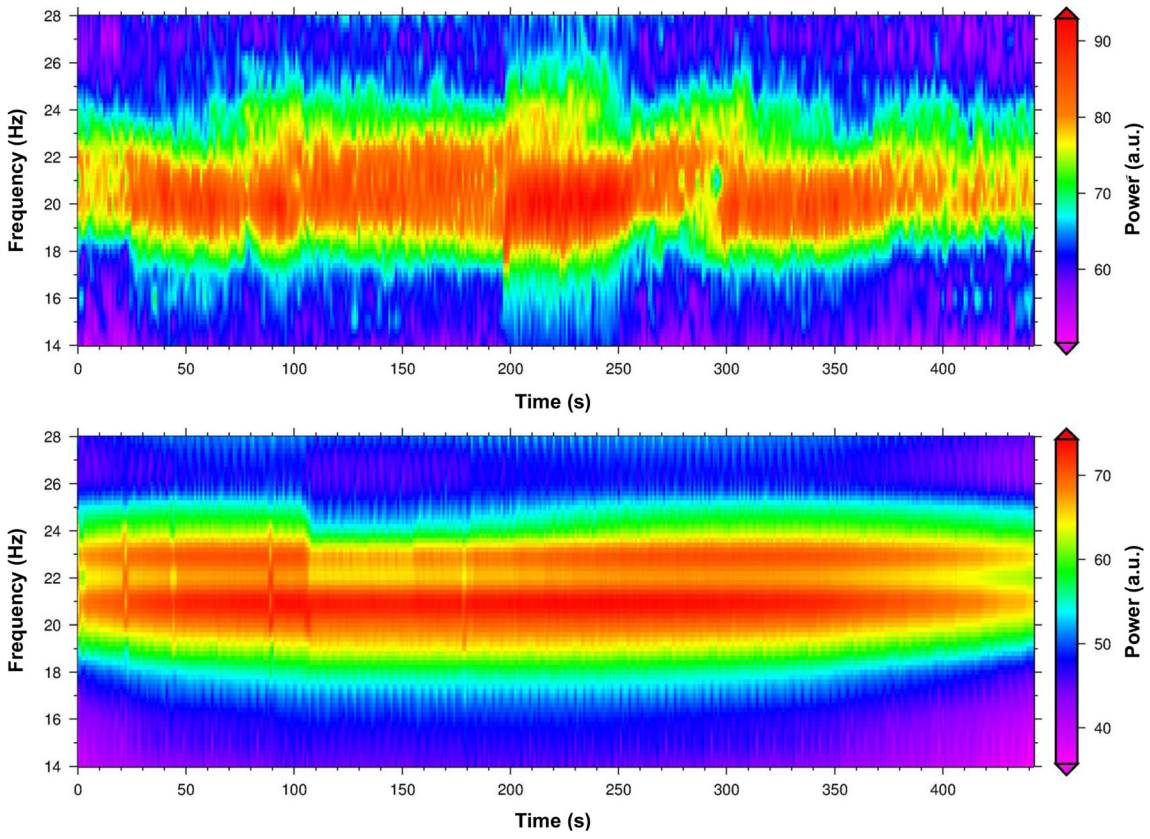

FIG. 10. (Color online) Smoothed spectrograms of the observed fin whale bout in the Z-channel (top) and the model for a source depth at 72 m (bottom).

https://doi.org/10.1121/10.0002426

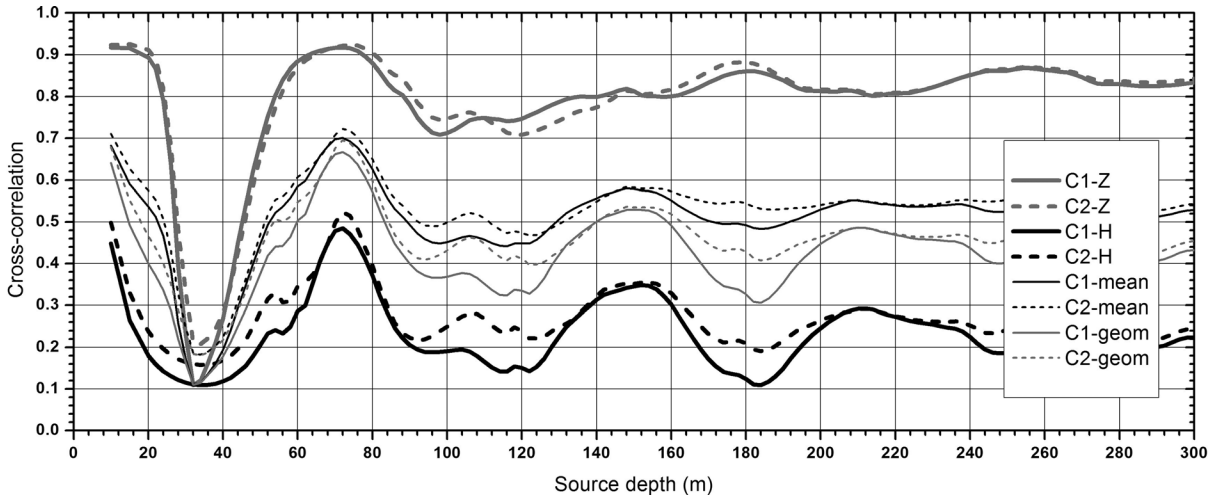

FIG. 11. Spectrogram correlation for the H-channel (bottom pair in black) and the Z-channel (top pair in grey). Middle set of curves show the four possible combinations between C1 and C2, and two ways of computing an average of spectrogram correlation, arithmetic and geometric.

a systematic bias on the estimated slant ranges, the model generation and spectrogram correlation was repeated for the H-channel with all slant ranges biased by +400 m or by −400 m. Some visible differences were seen in the resulting spectrograms, though the overall interference pattern remained similar to previous results for a 72 m source depth (Fig. 12).

Next, the spectrogram correlations C1 and C2 between the observed spectrogram and models computed with the biased slant range for the H-channel were calculated. Regarding the negatively biased set of slant ranges, the best source depths found were 68 m for C1 and 70 m for C2. For the positively biased set of slant ranges, the best source depths found were 74 m for both C1 and C2. These results confirmed that in the investigated bout we can infer that the uncertainty on the source depth, taking all possible constraints, was ±2 m.

IV. DISCUSSION

LME used passive acoustic monitoring (PAM) to provide a non-intrusive approach for estimating the depth at which a fin whale is producing 20-Hz notes. When compared to Charif *et al.* (2002), this study and the proposed methodology showed that LME can be used also with a single receiver.

For deep water conditions, the results showed that the LME interference patterns were rare for shallow source depths (<100 m), and appeared only at some limited slant ranges. Furthermore, the recordings of acoustic pressure from the hydrophone channel did not show any LME for source depths shallower than 50 m and slant ranges larger than 5000 m (Fig. 5). For shorter slant ranges, LME could be seen by hydrophone recordings for source depths deeper than 30 m. However, due to the reverse surface reflection coefficient, the Z-channel data showed LME at shallow source depths and short slant ranges. The results demonstrated that the joint use of Z- and H-channel data greatly improved the usefulness of the LME spectrograms to estimate sound source depth. To investigate the possible use of LME to estimate the source depth of a vocalizing fin whale, one bout that lasted almost 3 h was selected for analysis. For the computed slant ranges of the fin whale notes, which varied between 6 and 12 km, an average source depth of 72 m was estimated. At this depth and slant range interval, the LME pattern in the model spectrograms was only clearly seen on the acoustic pressure recordings from the H-channel, while the results for the Z-channel were more ambiguous.

The spectrogram correlation plots that screened all possible models with a source depth from 10–300 m every 2 m showed that the estimated depth value was very well defined, so that a maximum uncertainty could be estimated to ±2 m. The results were confirmed by visual inspection, but two features require additional discussion. First, the best model LME spectrogram for the H-channel did not explain the destructive interference that was observed between 210 and 220 s (pseudo-time) (Fig. 8). Matias and Harris (2015) showed that for a sensor placed at the seafloor, such as an OBS, the hydrophone and vertical seismometer recordings are disturbed at slant ranges close to the critical range for a sound wave incident at the seafloor because they both have small amplitudes. In addition, beyond the critical range, phase shifts and deformation of the signals occur for the Z-channel. Using 1500 m/s for the sound speed in water and 1800 m/s for the P-wave velocity in the shallow sediments that cover the Gulf of Cadiz, the critical range is 7300 m, coinciding with the slant ranges computed for the fin whale notes used in this study. Since this effect was not as clear on the Z-channel, the results suggest that the disturbances expected at the critical range affected the Z- and H-channels differently. Another hypothesis is that the true source depth was different from the 72 m estimated. Testing for the effects of a systematic bias in slant range in the depth estimates showed that there was a small uncertainty of ±2 m. Second, the spectrogram correlation plots still showed a

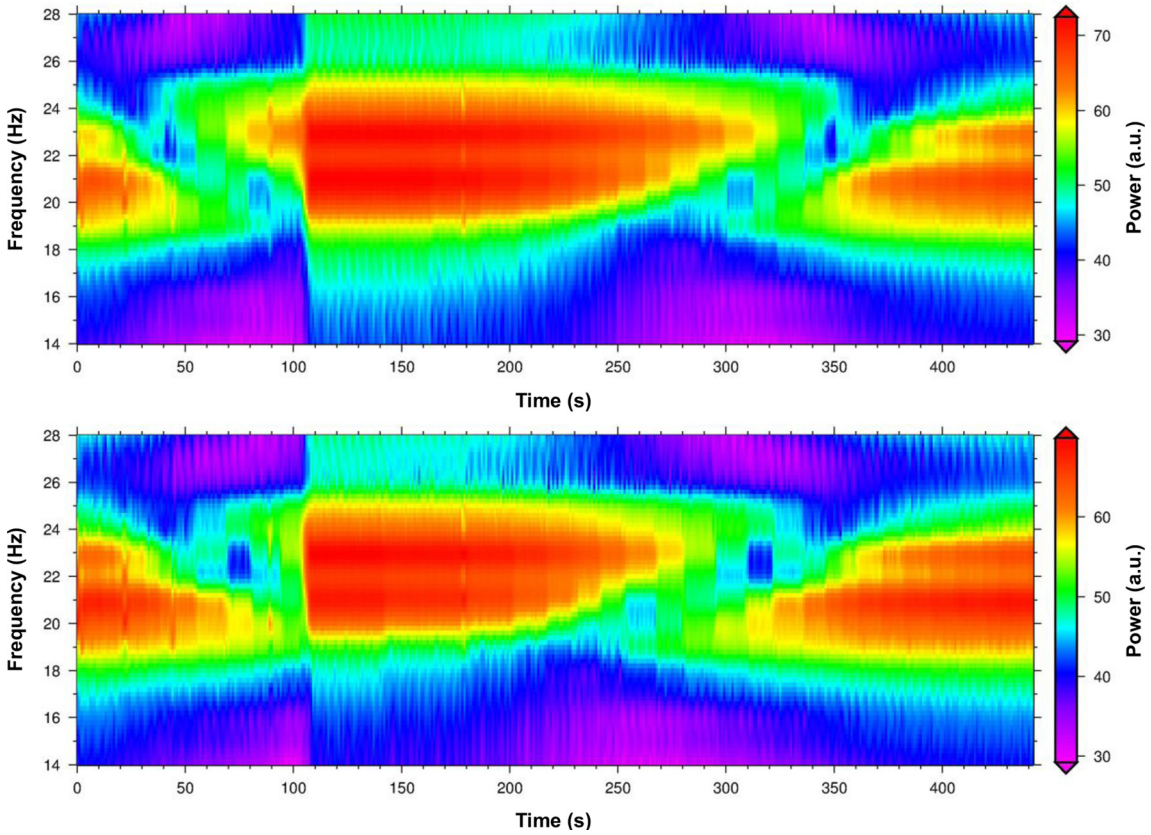

FIG. 12. (Color online) Model spectrograms computed for two different sets of ranges for the H-channel: i) measured – 400 m (top); ii) measured + 400 m (bottom), source depth at 72 m.

high value of correlation for shallow source depths of 10 m for which the models showed no LME interference. Rescaling the spectrogram grids helped, but did not completely resolve, this situation. Since the final solution should be checked by visual inspection, the shallow solution models were easily discarded. For the conditions investigated in this study, the method was reliable only for source depths greater than 20 m.

To explore the use of LME method to estimate the source depth in this study, the diving depth of the fin whale was assumed to be the same during the 3 h of the bout, which comprised 10 vocalizing dives, 6 of them complete. These complete dives were very stereotyped in terms of their duration, even when they were 2 h apart. Tag data show a general "U" shape diving profile for fin whales, whether they are performing lunge-feeding behavior (Croll *et al.*, 2001; Goldbogen *et al.*, 2012), or a non-foraging dive (Croll *et al.*, 2001; Stimpert *et al.*, 2015). When fin whales perform non-foraging dives, they stay at a certain depth for a period of time and then come back to the surface. Results from Stimpert *et al.* (2015) further displayed similar "U" pattern in dive of vocalizing and non-vocalizing individuals. Blue whales also call at a consistent depth across a series of dives (Oleson *et al.*, 2007). All of the above arguments support the assumption that the diving depth of a fin whale may be treated as constant on the successive vocalizing dives that comprise one bout.

Information about sound production in mysticetes is still limited, compared with the knowledge available for odontocetes (Au *et al.*, 2000). Currently, only Stimpert *et al.* (2015) provide measurements of the depth at which fin whales produce 20-Hz notes. Estimates of depths of vocalizing fin whales are also available from acoustic recordings associated with visual observations in Watkins *et al.* (1987), and with sound propagation models in Širović *et al.* (2007) and Weirathmueller *et al.* (2013). The acoustic recording tag data in Stimpert *et al.* (2015) show that when fin whales are producing 20-Hz notes, they usually perform short dives to shallow depths at 15–20 m. The maximum source depth they reported for a vocalizing fin whale was about 95 m in the Southern California Bight (Stimpert *et al.*, 2015). The estimated source depth of 72 m for the vocalizing fin whale investigated in this study was deeper than the average depths reported for vocalizing fin whales, but it was still within the range of the reported values (Watkins *et al.*, 1987; Širović *et al.*, 2007; Weirathmueller *et al.*, 2013; Stimpert *et al.*, 2015) and below the maximum vocalization depth of 220 m predicted with a model of sound production for blue whales (Aroyan *et al.*, 2000), which also produce low frequency and high source level sounds (Cummings and Thompson, 1971). Although cetaceans do not need to open their mouths or their blowholes to produce sound, like terrestrial animals, they still use air as its driving force, which is inherited from their terrestrial ancestors (Tyack, 2000). Vibrations of the

https://doi.org/10.1121/10.0002426

soft tissues, produced by the passing of the air under pressure, transfer to the water as sound pressure waves (Tyack, 2000). Aroyan *et al.* (2000) modelled sound production in blue whales, and argued that whales need a certain flow volume of air in order to vocalize, and that the compression of gas with depth limits the depth at which baleen whales can vocalize.

Therefore, while physiological aspects likely limit the maximum depth at which whales vocalize, preferences of depth for sound production can be influenced by sound propagation properties and energetic efficiency (Williams *et al.*, 2000; Oleson *et al.*, 2007; Stimpert *et al.*, 2015). The sound speed profile calculated from the CTD data used in this study showed a steep change in the sound speed between depths of 40 and 70 m (see supplementary Fig. 3[1]), as a result of changes in the water density. This layer is also referred to as pycnocline, and can cause the formation of ducts that trap sound and improve long distance sound propagation (Molland, 2008; Stimpert *et al.*, 2015). In the Gulf of Cadiz, fin whales might dive to the depths of this pycnocline to maximize the reach of their low frequency sounds. During the production of sounds, whales also consume energy to swim. To conserve energy during the performance of these two behaviors, Oleson *et al.* (2007) suggested that blue whales could dive to depths of 20–30 m, where they could have neutral buoyancy, and remain at these depths without actively swimming while producing sounds. In the case of the estimated sound source depth of 72 m presented in our study, the vocalizing whale would have a negative buoyancy. In Sec. I, the hypothesis that fin whales might select a depth for vocalizing that improves sound propagation by reducing TL was presented. The BELLHOP sound propagation model was used to test whether sound source depth of the whale studied here could minimize the TL of a 20-Hz fin whale note in the ocean environment. The propagation of a source frequency of 22 Hz, which is the middle frequency of 20-Hz fin whale notes (Širović *et al.*, 2007), produced at two source depths, 20 and 72 m, and over a 200 km range was modelled. The receiver was assumed to be 5 m deep and the sound speed profile mentioned in Sec. II was also used. The models showed large differences in TL values for short ranges (<14 km), with calling at 20 m leading to 20–40 dB reduction in TL compared to 72 dB. For ranges over 14 km, the median difference in TL between the two models was 4.48 dB for 1 m (SD 6.79), which might not represent a significant difference. Further estimates of the depth of vocalizing fin whales in the Gulf of Cadiz using the LME interference pattern and measurements of contemporary sound speed profiles need to be undertaken to assess whether the depth distribution of vocalizing whales may be selected to improve sound propagation for specific expected ranges of recipients.

V. CONCLUSIONS

Fin whales produce sequences of stereotyped 20-Hz notes that may last for several hours. When 20-Hz notes are formed into a composite spectrogram that disregards the periods of silence, clear interference patterns could be identified, and they could be interpreted as a result of LME. When the sound is recorded at the sea bottom (e.g., with an OBS), LME results from the superposition of the direct path and the sea surface reflection. For receivers suspended above the sea bottom, another interference results from the sound paths reflected off the seafloor that must also be considered when using LME. LME interference varies as a function of signal frequency, source depth, and slant range. The pattern of LME interference recorded on an OBS also depends on the channel that is being used, i.e., the sound pressure recorded by a hydrophone or the vertical particle velocity recorded by the vertical channel of the seismometer. For the deep water conditions found in the Gulf of Cadiz, the area of this study, pressure recordings were predicted to only detect LME in cases where source depths were deeper than 30 m and slant ranges greater than 5000 m, while predictions using ground motion recordings made by the vertical seismometer channel were most suitable for shallower source depths and shorter slant ranges. The results of this study showed that the joint use of the two channels improves the overall correlation between observed and the best fit model spectrogram.

The use of LME to infer source depth requires availability of a good estimate of the slant range. This study showed that this parameter can be obtained from single sensor channel recordings, even when the multipath signal is barely seen on the recordings and cannot be automatically or manually detected. The enhancement of the multipath signals can be obtained processing the sequence of notes as a seismic profile using standard processing routines. LME can be used in other recording settings by single sensor or multiple sensors. Synthetic models show that a large set of slant ranges should be explored, either by one sensor (preferably with Z- and H-channels) or by multiple sensors recording the same bout. When multiple sensor recordings are available, an estimate of the diving depth can be derived for each dive (assuming a "U" shape), instead of an average diving depth for the whole bout as was done in this work.

ACKNOWLEDGMENTS

The acoustic data were collected for the NEAREST project, on behalf of the EU Specific Programme "Integrating and Strengthening the European Research Area," Sub-Priority 1.1.6.3, "Global Change and Ecosystems," Contract No. 037110. The data analysis was carried out as part of the Ph.D. thesis by A.P. The thesis was funded by Fundação para a Ciência e a Tecnologia, through a Ph.D. scholarship SFRH/BD/52554/2014, from the Doctoral Programme – PD/143/2012 – Lisbon Doctoral School on Earth System Science, Instituto Dom Luiz (IDL). A.P. was also funded by the Project AWARENESS (PTDC/BIA-BMA/30514/201) and FCT through project UIDB/50019/2020 – IDL. D.H. was funded by the Office of Naval Research (ONR) (Award: N00014-14-1-0394) and P.T.

from ONR Award N00014-18-1-2062. PLT also acknowledges the support of the MASTS pooling initiative (The Marine Alliance for Science and Technology for Scotland) in the completion of this study. MASTS is funded by the Scottish Funding Council (grant reference HR09011) and contributing institutions. The authors would like to thank two anonymous reviewers for their valuable comments and suggestions that improved the manuscript.

[1]See supplementary material at https://www.scitation.org/doi/suppl/10.1121/10.0002426 for an example of the results of the interaction between the direct and the multipaths of a synthetic 20-Hz fin whale noted at different slant ranges.

Aroyan, J. L., McDonald, M. A., Webb, S. C., Hildebrand, J. A., Clark, D., Laitman, J. T., and Reidenberg, J. S. (**2000**). "Acoustic models of sound production and propagation," in *Hearing by Whales and Dolphins*, edited by W. W. L. Au, A. N. Popper, and R. R. Fay (Springer, New York, NY), pp. 409–469.

Au, W. W. L., and Hastings, M. C. (**2008**). *Principles of Marine Bioacoustics* (Springer-Verlag, New York, NY).

Au, W. W. L., Popper, A. N., and Fay, R. R. (**2000**). *Hearing by whales and dolphins* (Springer, New York, NY).

Booij, N., Ris, R. C., and Holthuijsen, L. H. (**1999**). "A third generation wave model for coastal region 1. Model description and validation," J. Geophys. Res. **10**, 7649–7666, https://doi.org/10.1029/98JC02622.

Brekhovskikh, L., and Lysanov, Y. (**1982**). *Fundamentals of Ocean Acoustics*. (Springer-Verlag, Berlin).

Castellote, M., Clark, C. W., and Lammers, M. O. (**2012**). "Fin whale (*Balaenoptera physalus*) population identity in the western Mediterranean Sea," Mar. Mamm. Sci. **28**, 325–344.

Charif, R. A., Mellinger, D. K., Dunsmore, K. J., Fristrup, K. M., and Clark, C. W. (**2002**). "Estimated sound source levels of fin whale (*Balaenoptera physalus*) vocalizations: Adjustments for surface interference," Mar. Mamm. Sci. **18**, 81–98.

Clark, C. W., Borsani, F., and Notarbartolo di Sciara, G. (**2002**). "Vocal activity of fin whales, *Balaenoptera physalus*, in the Ligurian Sea," Mar. Mamm. Sci. **18**, 281–285.

Clark, C. W., Ellison, W. T., Southall, B. L., Hatch, L., Van Parijs, S. M., Frankel, A., and Ponirakis, D. (**2009**). "Acoustic masking in marine ecosystems: Intuitions, analysis, and implication," Mar. Ecol. Prog. Ser. **395**, 201–222.

Croll, D. A., Acevedo-Gutiérrez, A., Tershy, B. R., and Urbán-Ramírez, J. (**2001**). "The diving behavior of blue and fin whales: Is dive duration shorter than expected based on oxygen stores?" Comp. Biochem. Physiol. A Mol. Integr. Physiol. **129**, 797–809.

Croll, D., Clark, C. W., Acevedo, A., Tershy, B., Flores, S., Gedamke, J., and Urban, J. (**2002**). "Only male fin whales sing loud songs," Nature **417**, 809.

Cummings, W. C., and Thompson, P. O. (**1971**). "Underwater sounds from the blue whale, *Balaenoptera musculus*," J. Acoust. Soc. Am. **50**, 1193–1198.

Delarue, J., Todd, S., Parijs, S. V., and Iorio, L. D. (**2009**). "Geographic variation in Northwest Atlantic fin whale (*Balaenoptera physalus*) song: Implications for stock structure assessment," J. Acoust. Soc. Am. **125**, 1774–1782.

Erbe, C., Reichmuth, C., Cunningham, K., Lucke, K., and Dooling, R. (**2016**). "Communication masking in marine mammals: A review and research strategy," Mar. Pollut. Bull. **103**, 15–38.

Etter, P. C. (**1995**). *Underwater Acoustic Modeling: Principles, Techniques and Applications*, 2nd ed. (CRC Press, London).

Geissler, W. H., Matias, L., Stich, D., Carrilho, F., Jokat, W., Monna, S., IbenBrahim, A., Mancilla, F., Gutscher, M.-A., Sallarès, V., and Zitellini, N. (**2010**). "Focal mechanisms for subcrustal earthquakes in the Gulf of Cadiz from a dense OBS deployment," Geophys. Res. Lett. **37**, L18309, https://doi.org/10.1029/2010GL044289.

Goldbogen, J. A., Calambokidis, J., Croll, D., McKenna, M. F., Potvin, J., Pyenson, N. D., Schorr, G., Shadwick, R. E., and Tershy, B. R. (**2012**). "Scaling of lunge feeding performance in rorqual whales: Mass-specific energy expenditure increases with body size and progressively limits diving capacity," Funct. Ecol. **26**, 216–226.

Harris, D., Matias, L., Thomas, L., Harwood, J., and Geissler, W. H. (**2013**). "Applying distance sampling to fin whale calls recorded by single seismic instruments in the Northeast Atlantic," J. Acoust. Soc. Am. **134**, 3522–3535.

Hatch, L. T., and Clark, C. W. (**2004**). "Acoustic differentiation between fin whales in both the North Atlantic and North Pacific Oceans, and integration with genetic estimates of divergence," Paper presented to the IWC Scientific Committee, Sorrento, Italy, July, Paper No. SC/56/SD6, pp. 1–37.

Hildebrand, J. A. (**2009**). "Anthropogenic and natural sources of ambient noise in the ocean," Mar. Ecol. Prog. Ser. **395**, 5–20.

Holthuijsen, L. H. (**2010**). *Waves in Oceanic and Coastal Waters* (Cambridge University Press, Cambridge).

Hovem, J. M. (**2013**). "Ray trace modeling of underwater sound propagation," in *Modeling and Measurement Methods for Acoustic Waves and for Acoustic Microdevices*, edited by Marco G. Beghi (IntechOpen, DOI: 10.5772/55935). Available at https://www.intechopen.com/books/modeling-and-measurement-methods-for-acoustic-waves-and-for-acoustic-microdevices/ray-trace-modeling-of-underwater-sound-propagation. (Last viewed March 30, 2020).

Hudson, R. F. (**1983**). "A horizontal range vs. depth solution of sound source position under general sound velocity conditions using the Lloyd's Mirror interference pattern," M.Sc. thesis, Naval Postgraduate School.

Kerman, B. R. (**1988**). *Sea Surface Sound: Natural Mechanisms of Surface Generated Noise in the Ocean*(Kluwer Academic Publishers, Dordrecht).

Kunc, H. P., McLaughlin, K. E., and Schmidt, R. (**2016**). "Aquatic noise pollution: Implications for individuals, populations, and ecosystems," Proc. R. Soc. Lond. B Biol. Sci. **283**, 20160839.

Lobue, N. (**2012**). (personal communication).

Lurton, X. (**2002**). *An Introduction to Underwater Acoustics* (Springer-Verlag, Berlin).

Marques, T. A., Thomas, L., Martin, S. W., Mellinger, D. K., Ward, J., Moretti, D., Harris D., and Tyack, P. (**2013**). "Estimating animal population density using passive acoustics," Biol. Rev. **88**, 287–309.

MathWorks. (**2010**). *Matlab, Version 7.10, computer software* (The Mathworks, Inc., Natick, MA).

Matias, L., and Harris, D. (**2015**). "A single-station method for the detection, classification and location of fin whale calls using ocean-bottom seismic stations," J. Acoust. Soc. Am. **138**, 504–520.

McDonald, M. A., Hildebrand, J. A., and Webb, S. C. (**1995**). "Blue and fin whales observed on a seafloor array in the Northeast Pacific," J. Acoust. Soc. Am. **98**, 712–721.

McDonald, M. A., Mesnick, S. L., and Hildebrand, J. A. (**2006**). "Biogeographic characterisation of blue whale songs worldwide: Using song to identify populations," J. Cetacean Res. Manag. **8**, 55–65.

Mellinger, D. K. (**2015**). (personal communication).

Molland, A. F. (**2008**). *The Maritime Engineering Reference Book: A Guide to Ship Design, Construction and Operation* (Elsevier, Oxford).

Northrop, J., Cummings, W. C., and Thompson, P. O. (**1968**). "20 Hz signals observed in the central Pacific," J. Acoust. Soc. Am. **43**, 383–384.

Oleson, E. M., Calambokidis, J., Burgess, W. C., McDonald, M. A., LeDuc, C. A., and Hildebrand, J. A. (**2007**). "Behavioral context of call production by eastern North Pacific blue whales," Mar. Ecol. Prog. Ser. **330**, 269–284.

Oleson, E. M., Širović, A., Bayless, A. R., and Hildebrand, J. A. (**2014**). "Synchronous seasonal change in fin whale song in the North Pacific," PLoS One **9**, e115678.

Parallel Geoscience. (**1999**). "SPW — Parallel seismic processing" (Incline Village, NV). Available at http://www.parallelgeo.com/?q=product&p=SPW (Last viewed March 30, 2020).

Parks, S. E., Clark, C. W., and Tyack, P. L. (**2007**). "Short- and long-term changes in right whale calling behavior: The potential effects of noise on acoustic communication," J. Acoust. Soc. Am. **122**, 3725–3731.

Parks, S. E., Searby, A., Celerier, A., Johnson, M., Nowacek, D. P., and Tyack, P. (**2011**). "Sound production behavior of individual North Atlantic right whales: Implications for passive acoustic monitoring," Endanger. Species Res. **15**, 63–76.

Payne, R. S., and Webb, D. (**1971**). "Orientation by means of long range acoustic signaling in baleen whales," Ann. N. Y. Acad. Sci. **188**, 110–141.

Pereira, A., Harris, D., Tyack, P., and Matias, L. (**2016**). "Lloyd's mirror effect in fin whale calls and its use to infer the depth of vocalizing animals," Proc. Meet. Acoust. **27**, 070002.
Pereira, A., Harris, D., Tyack, P., and Matias, L. (**2020**). "Fin whale acoustic presence and song characteristics in seas to the southwest of Portugal," J. Acoust. Soc. Am. **147**, 2235–2249.
Premus, V., and Spiesberger, J. L. (**1997**). "Can acoustic multipath explain finback (*B. physalus*) 20-Hz doublets in shallow water?," J. Acoust. Soc. Am. **101**, 1127–1138.
Richardson, W. J., Greene, J. C. R., Malme, C. I., and Thomson, D. H. (**1995**). *Marine Mammals and Noise* (Academic Press, San Diego, CA).
Silva, S. D. M. M. F. (**2017**). "Strain partitioning and the seismicity distribution within a transpressive plate boundary: SW Iberia-NW Nubia," Ph.D. dissertation, University of Lisbon, Lisbon, Portugal.
Širović, A., Hildebrand, J. A., and Wiggins, S. M. (**2007**). "Blue and fin whale call source levels and propagation range in the Southern Ocean," J. Acoust. Soc. Am. **122**, 1208–1215.
Soule, D. C., and Wilcock, W. S. D. (**2013**). "Fin whale tracks recorded by a seismic network on the Juan de Fuca Ridge, Northeast Pacific Ocean," J. Acoust. Soc. Am. **133**, 1751–1761.
Stimpert, A. K., DeRuiter, S. L., Falcone, E. A., Joseph, J., Douglas, A. B., Moretti, D. J., Friedlaender, A. S., Calambokidis, J., Gailey, G., Tyack, P. L., and Goldbogen, J. A. (**2015**). "Sound production and associated behavior of tagged fin whales (*Balaenoptera physalus*) in the Southern California Bight," Anim. Biotelemetry **3**, 23.
Thode, A., Mellinger, D. K., Stienessen, S., Martinez, A., and Mullin, K. (**2002**). "Depth-dependent acoustic features of diving sperm whales (*Physeter macrocephalus*) in the Gulf of Mexico," J. Acoust. Soc. Am. **112**, 308–321.
Thompson, S. R. (**2009**). "Sound propagation considerations for a deep-ocean acoustic network," M.Sc. thesis, Naval Postgraduate School.
Tyack, P. L. (**1997**). "Development and social functions of signature whistles in bottlenose dolphins, *Tursiops truncatus*," Bioacoustics **8**, 21–46.
Tyack, P. L. (**2000**). "Functional aspects of cetacean communication," in *Cetacean Societies: Field Studies of Dolphins and Whales*, edited by J. Mann, R. C. Connor, P. L. Tyack, and H. Whitehead (The University of Chicago Press, Chicago, IL), pp. 270–307.
Urick, R. J. (**1967**). *Principles of Underwater Sound for Engineers* (McGraw-Hill Education, New York, NY).
Wang, D., Huang, W., Garcia, H., and Ratilal, P. (**2016**). "Vocalization source level distributions and pulse compression gains of diverse baleen whale species in the Gulf of Maine," Remote Sens. **8**, 881.
Watkins, W. A. (**1981**). "Activities and underwater sounds of fin whales," Sci. Rep. Whales Res. Inst. **33**, 83–117.
Watkins, W. A., Tyack, P., Moore, K. E., and Bird, J. E. (**1987**). "The 20-Hz signals of finback whales (*Balaenoptera physalus*)," J. Acoust. Soc. Am. **82**, 1901–1912.
Weirathmueller, M. J., Stafford, K. M., Wilcock, W. S. D., Hilmo, R. S., Dziak, R. P., and Tréhu, A. M. (**2017**). "Spatial and temporal trends in fin whale vocalizations recorded in the NE Pacific Ocean between 2003-2013," PLoS One **12**, e018612.
Weirathmueller, M. J., Wilcock, W. S. D., and Soule, D. C. (**2013**). "Source levels of fin whale 20-Hz pulses measured in the Northeast Pacific Ocean," J. Acoust. Soc. Am. **133**, 741–749.
Wiggins, S. M., Roch, M. A., and Hildebrand, J. A. (**2010**). "TRITON software package: Analyzing large passive acoustic monitoring data sets using MATLAB," J. Acoust. Soc. Am. **128**, 2299.
Wilcock, W. S. D. (**2012**). "Tracking fin whales in the northeast Pacific Ocean with a seafloor seismic network," J. Acoust. Soc. Am. **132**, 2408–2419.
Williams, T. M., Davis, R. W., Fuiman, L. A., Francis, J., LeBoeuf, B. J., Horning, M., Calambokidis, J., and Croll, D. A. (**2000**). "Sink or swim: Strategies for cost-efficient diving by marine mammals," Science **288**, 133–136.
Zitellini, N., Gràcia, E., Matias, L., Terrinha, P., Abreu, M. A., DeAlteriis, G., Henriet, J. P., Dañobeitia, J. J., Masson, D. G., Mulder, T., Ramella, R., Somoza, L., and Diez, S. (**2009**). "The quest for the Africa–Eurasia plate boundary west of the Strait of Gibraltar," Earth Planet. Sci. Lett. **280**, 13–50.